

Equilibrium climate sensitivity estimated by equilibrating climate models

Article

Accepted Version

Rugenstein, M., Bloch-Johnson, J. ORCID:
<https://orcid.org/0000-0002-8465-5383>, Gregory, J. ORCID:
<https://orcid.org/0000-0003-1296-8644>, Andrews, T.,
Mauritsen, T., Li, C., Frölicher, T. L., Paynter, D., Danabasoglu,
G., Yang, S., Dufresne, J.-L., Cao, L., Schmidt, G. A., Abe-
Ouchi, A., Geoffroy, O. and Knutti, R. (2020) Equilibrium
climate sensitivity estimated by equilibrating climate models.
Geophysical Research Letters, 47 (4). e2019GL083898. ISSN
0094-8276 doi: 10.1029/2019GL083898 Available at
<https://centaur.reading.ac.uk/87462/>

It is advisable to refer to the publisher's version if you intend to cite from the work. See [Guidance on citing](#).

To link to this article DOI: <http://dx.doi.org/10.1029/2019GL083898>

Publisher: American Geophysical Union

All outputs in CentAUR are protected by Intellectual Property Rights law,
including copyright law. Copyright and IPR is retained by the creators or other
copyright holders. Terms and conditions for use of this material are defined in
the [End User Agreement](#).

www.reading.ac.uk/centaur

CentAUR

Central Archive at the University of Reading

Reading's research outputs online

Equilibrium climate sensitivity estimated by equilibrating climate models

Maria Rugenstein^{1,2*}, Jonah Bloch-Johnson³, Jonathan Gregory^{3,4}, Timothy Andrews⁴, Thorsten Mauritsen⁵, Chao Li², Thomas L. Frölicher^{6,7}, David Paynter⁸, Gokhan Danabasoglu⁹, Shuting Yang¹⁰, Jean-Louis Dufresne¹¹, Long Cao¹², Gavin A. Schmidt¹³, Ayako Abe-Ouchi¹⁴, Olivier Geoffroy¹⁵, and Reto Knutti¹

¹Institute for Atmospheric and Climate Science, ETH Zurich, CH-8092 Zurich, Switzerland

²Max-Planck-Institute for Meteorology, Bundesstrasse 53, 20146 Hamburg, Germany

³NCAS, University of Reading, Reading

⁴UK Met Office Hadley Centre, FitzRoy Road, Exeter, EX1 3PB

⁵Stockholm University, SE-106 91 Stockholm, Sweden

⁶Climate and Environmental Physics, Physics Institute, University of Bern, Switzerland

⁷Oeschger Centre for Climate Change Research, University of Bern, Switzerland

⁸Geophysical Fluid Dynamics Laboratory, Princeton, New Jersey, USA

⁹National Center for Atmospheric Research, P.O. Box 3000, Boulder, CO 80307

¹⁰Danish Meteorological Institute, Lyngbyvej 100, DK-2100 Copenhagen, Denmark

¹¹LMD/IPSL, Centre National de la Recherche Scientifique, Sorbonne Université, École Normale

Supérieure, PSL Research University, École Polytechnique, Paris, France

¹²School of Earth Sciences, Zhejiang University, Hang Zhou, Zhejiang Province, 310027, China

¹³NASA Goddard Institute for Space Studies, 2880 Broadway, New York, NY 10025

¹⁴Atmosphere and Ocean Research Institute, The University of Tokyo, Japan

¹⁵Centre National de Recherches Météorologiques, Université de Toulouse, Météo-France, CNRS,

Toulouse, France

Key Points:

- 27 simulations of 15 general circulation models are integrated to near equilibrium
- All models simulate a higher equilibrium warming than predicted by using extrapolation methods
- Tropics and mid-latitudes dominate the change of the feedback parameter on different timescales

*Max-Planck-Institute for Meteorology, Bundesstrasse 53, 20146 Hamburg, Germany

Corresponding author: Maria Rugenstein, maria.rugenstein@mpimet.mpg.de

31 **Abstract**

32 The methods to quantify equilibrium climate sensitivity are still debated. We collect
 33 millennial-length simulations of coupled climate models and show that the global mean equi-
 34 librium warming is higher than those obtained using extrapolation methods from shorter
 35 simulations. Specifically, 27 simulations with 15 climate models forced with a range of CO₂
 36 concentrations show a median 17% larger equilibrium warming than estimated from the first
 37 150 years of the simulations. The spatial patterns of radiative feedbacks change continu-
 38 ously, in most regions reducing their tendency to stabilizing the climate. In the equatorial
 39 Pacific, however, feedbacks become more stabilizing with time. The global feedback evo-
 40 lution is initially dominated by the tropics, with eventual substantial contributions from
 41 the mid-latitudes. Time-dependent feedbacks underscore the need of a measure of climate
 42 sensitivity that accounts for the degree of equilibration, so that models, observations, and
 43 paleo proxies can be adequately compared and aggregated to estimate future warming.

44 **1 Estimating equilibrium climate sensitivity**

45 The equilibrium climate sensitivity (ECS) is defined as the global- and time-mean,
 46 surface air warming once radiative equilibrium is reached in response to doubling the atmo-
 47 spheric CO₂ concentration above pre-industrial levels. It is by far the most commonly and
 48 continuously applied concept to assess our understanding of the climate system as simulated
 49 in climate models and it is used to compare models, observations, and paleo-proxies (Knutti
 50 et al., 2017; Charney et al., 1979; Houghton et al., 1990; Stocker, 2013). Due to the large
 51 heat capacity of the oceans, the climate system takes millennia to equilibrate to a forcing,
 52 but performing such a long simulation with a climate model is often computationally not
 53 feasible. As a result, many modeling studies use extrapolation methods on short, typically
 54 150-year long, simulations to project equilibrium conditions (Taylor et al., 2011; Andrews
 55 et al., 2012; Collins et al., 2013; Otto et al., 2013; Lewis & Curry, 2015; Andrews et al.,
 56 2015; Forster, 2016; Calel & Stainforth, 2017). These so-called *effective* climate sensitiv-
 57 ities (Murphy, 1995; Gregory et al., 2004) are often reported as ECS values (Hargreaves
 58 & Annan, 2016; Tian, 2015; Brient & Schneider, 2016; Forster, 2016). Research provides
 59 evidence for decadal-to-centennial changes of feedbacks (e.g., Murphy (1995); Senior and
 60 Mitchell (2000); Gregory et al. (2004); Winton et al. (2010); Armour et al. (2013); Prois-
 61 totescu and Huybers (2017); Paynter et al. (2018)) but the behavior on longer timescales has

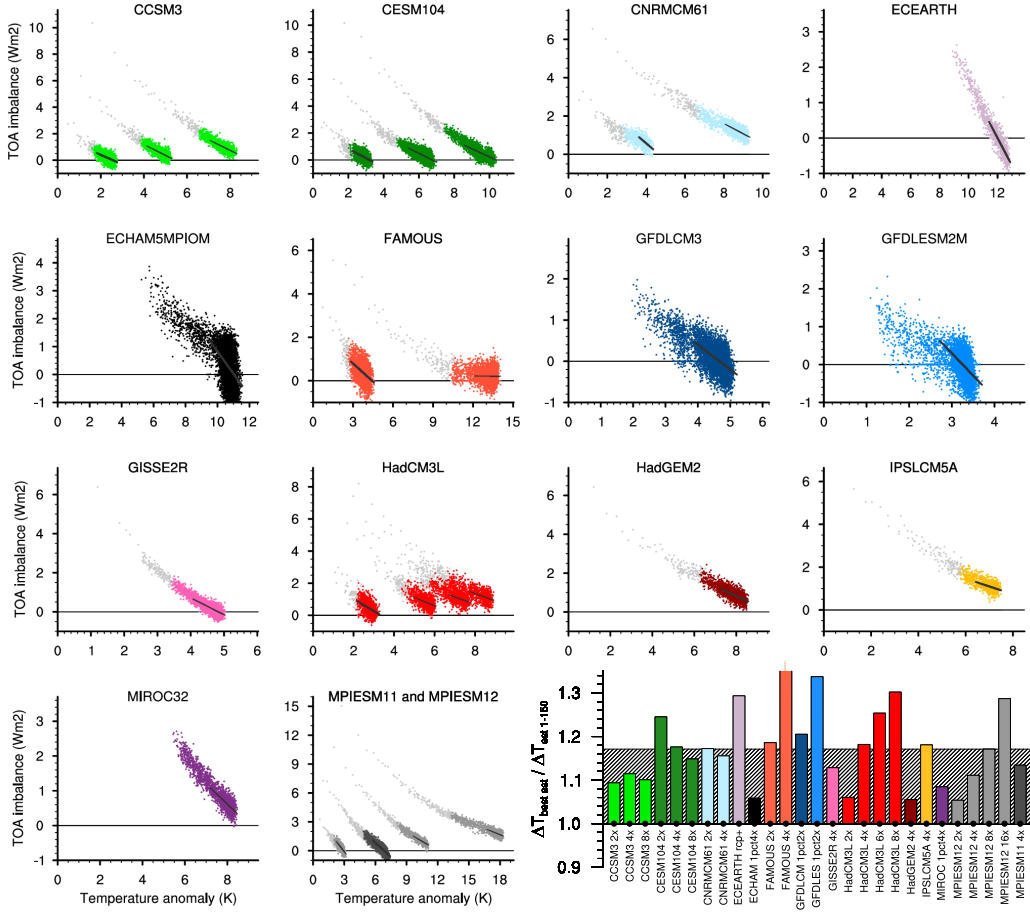


Figure 1. Evolution of global and annual mean top of the atmosphere (TOA) imbalance and surface temperature anomalies (14 small panels). The first 150 years of step forcing simulations are depicted in light gray. For experiments which are not step forcing simulations only the period after stabilizing CO₂ concentrations is shown. The black line shows the linear regression of TOA imbalance and surface warming for the last 15% of warming. The panel on the lower right shows the ratio $\Delta T_{\text{best est}} / \Delta T_{\text{est } 1-150}$, see text for definitions. A dot at the lower end of the bar indicates with 90% confidence that $\Delta T_{\text{best est}}$ and $\Delta T_{\text{est } 1-150}$ obtained by resampling 10,000 times do not overlap. The gray hashed bar in the background is the median of all simulations (1.17). FAMOUS *abrupt4x* ends outside of the depicted range at 1.53. Table 1 specifies the model versions and names, length of simulations, and numerical values for different climate sensitivity estimates.

not been compared among models. Here, we utilize LongRunMIP, a large set of millennial-long coupled general circulation models (GCMs) to estimate the true equilibrium warming, study the centennial-to-millennial behavior of the climate system under elevated radiative forcing, and test extrapolation methods. LongRunMIP is a model intercomparison project (MIP) of opportunity in that its initial contributions were preexisting simulations, without a previously agreed upon protocol. The minimum contribution is a simulation of at least 1000 years with a constant CO₂ forcing level. The collection consists mostly of doubling or quadrupling step forcing simulations (“abrupt2x”, “abrupt4x”, ...) as well as annual increments of 1% CO₂ increases reaching and sustaining doubled or quadrupled concentrations (“1pct2x”, “1pct4x”). Table 1 lists the simulations and models used here, while M. Rugenstein et al. (2019) documents the entire modeling effort and each contribution in detail.

The equilibration of top of the atmosphere (TOA) radiative imbalance and surface temperature anomaly of the simulations are depicted in Fig. 1. Throughout the manuscript, we show anomalies as the difference to the mean of the unforced control simulation with pre-industrial CO₂ concentrations. Light gray dots indicate annual means of the first 150 years of a step forcing simulation, requested by the Coupled Model Intercomparison Project Phase 5 and 6 protocols (CMIP5 and CMIP6; Taylor et al. (2011); Eyring et al. (2016)) and widely used to infer ECS (Andrews et al., 2012; Geoffroy, Saint-Martin, Olivié, et al., 2013). We refer to this timescale as “decadal to centennial”. Colors indicate the “centennial to millennial” timescale we explore here. The diminishing distances to the reference line at TOA = 0 indicate that most simulations archive near-equilibrium by the end of the simulations. However, even if a simulation has an equilibrated TOA imbalance of near zero, the surface temperature, surface heat fluxes, or ocean temperatures can still show a trend (discussed in M. Rugenstein et al. (2019)).

Throughout the manuscript, we use “ $\Delta T_{[specification]}$ ” for a true or estimated equilibrium warming, for a range of forcing levels not only CO₂ doubling (Table 1). We define the best estimate of equilibrium warming, $\Delta T_{best\ est}$, as the temperature-axis intersect of the regression of annual means of TOA imbalance and surface temperature anomaly over the simulations’ final 15% of global mean warming (black lines in Fig. 1). The lower right panel in Fig. 1 illustrates that all simulations eventually warm significantly more (measured by $\Delta T_{best\ est}$) than predicted by the most commonly used method to estimate the equilibrium temperature by extrapolating a least-square regression of the first 150 years of the same step forcing simulation (Gregory et al., 2004; Flato et al., 2013), denoted here as “ $\Delta T_{est\ 1-150}$ ”.

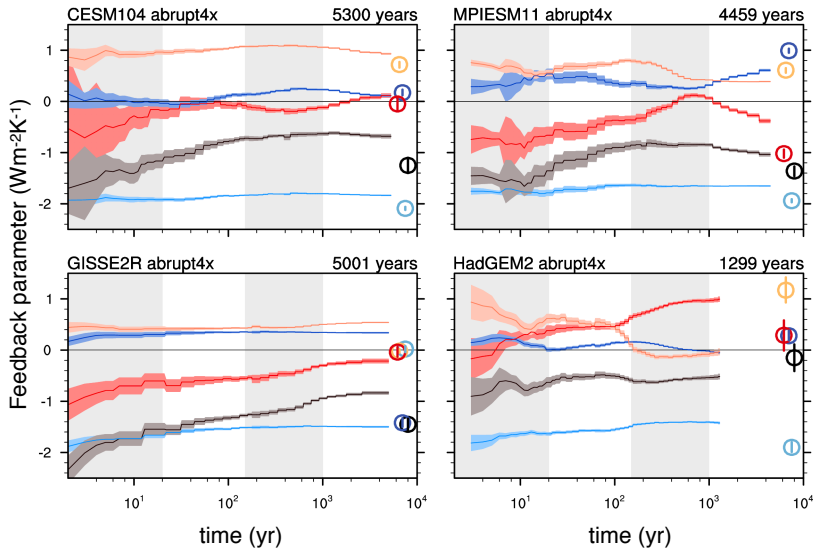
95 For simulations that have gradual forcings (e.g., *1pct2x*), we use 150 year long step forcing
 96 simulations of the same model to calculate $\Delta T_{est\ 1-150}$. The median increase of $\Delta T_{best\ est}$
 97 over $\Delta T_{est\ 1-150}$ is 17% for all simulations and 16% for the subset of CO₂ doubling and qua-
 98 drupling simulations. While $\Delta T_{est\ 1-150}$ implies a constant feedback parameter (the slope
 99 of the regression line), other extrapolation methods allow for a time-dependent feedback pa-
 100 rameter, but still typically underestimate $\Delta T_{best\ est}$: Using years 20-150 in linear regression
 101 ($\Delta T_{est\ 20-150}$; e.g., Andrews et al. (2015); Armour (2017)) results in a median equilibrium
 102 warming estimate which is 7% lower than $\Delta T_{best\ est}$, both for all simulations and the subset
 103 of CO₂ doubling and quadrupling. The two-layer model including ocean heat uptake efficacy
 104 ($\Delta T_{EBM-\epsilon}$; e.g., Winton et al. (2010); Geoffroy, Saint-Martin, Bellon, et al. (2013)) results
 105 in a multi model median equilibrium warming estimate which is 9% lower than $\Delta T_{best\ est}$,
 106 again both for all simulations and the subset of CO₂ doubling and quadrupling. Both meth-
 107 ods are described and illustrated in the supplemental material.

108 $\Delta T_{best\ est}$ of any forcing level can be scaled down to doubling CO₂ levels to estimate
 109 equilibrium warming for CO₂ doubling. We do so by assuming that the temperature scales
 110 with the forcing level, which depends logarithmically on the CO₂ concentration (Myhre et
 111 al., 1998), and assuming no feedback temperature dependence (e.g. Mauritsen et al. (2018)
 112 and Rohrschneider et al. (2019), see discussion below). The estimate of equilibrium warm-
 113 ing for CO₂ doubling range from 2.42 to 5.83 K (excluding FAMOUS *abrupt4x* at 8.55K;
 114 see Table 1 and Fig. 1). Note that the simulation *abrupt4x* of the model FAMOUS warms
 115 anomalously strongly. As this simulation represents a physically possible result, we do not
 116 exclude it from the analysis (see more details in SM Section 4). The results are qualitatively
 117 the same if $\Delta T_{best\ est}$ is defined by regressing over the last 20% instead of 15% of warming
 118 or instead time averaging the surface warming toward the end of every simulation without
 119 taking the information of the TOA imbalance into account. SM Section 1 discusses different
 120 options and choices to determine $\Delta T_{best\ est}$.

121 2 Global feedback evolution

122 Current extrapolation methods underestimate the equilibrium response because climate
 123 feedbacks change with the degree of equilibration (Murphy, 1995; Senior & Mitchell, 2000;
 124 Andrews et al., 2015; Knutti & Rugenstein, 2015; M. A. A. Rugenstein, Caldeira, & Knutti,
 125 2016; Armour, 2017; Proistosescu & Huybers, 2017; Paynter et al., 2018). We define the
 126 global net TOA feedback as the *local tangent* in temperature-TOA space ($\delta\text{TOA}/\delta T$) com-

a) Time evolution of feedbacks in four models



b) Feedback components for different time periods

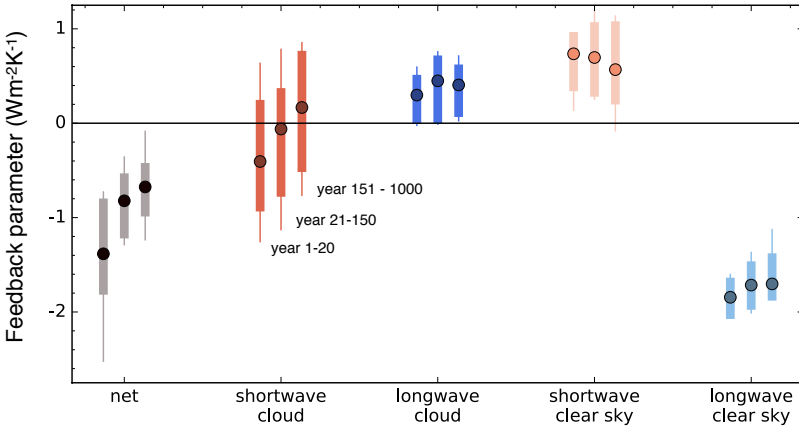


Figure 2. a) Time evolution of global feedbacks in four characteristic models. Net TOA feedback (gray) is the sum of its components: the cloud effects in the shortwave (red) and longwave (blue), and clear sky feedbacks in the shortwave (salmon) and longwave (light blue). Circles at the right of each panel indicate the feedbacks arising from internal variability; shading and vertical lines shows the 2.5-97.5% confidence intervals. Panel titles give the model name and length of the simulation. Time periods of 1-20 years and 150-1000 years are shaded gray. (b) Feedback evolution in the step forcing simulations of CCSM3, CESM104, CNRMCM6, ECHAM5MPIOM, FAMOUS, GISS-E2R, HadCM3L, HadGEM2, IPSLCM5A, MPIESM11, and MPIESM12, see Table 1 for naming convention. Lines show all simulations, dots represent median values and bars spans all but the two highest and two lowest simulations. SM Fig. 4 and 5 show the feedback evolution for all available simulations.

puted by a least square regression of all global and annual means of netTOA imbalance and surface temperature anomaly within a temperature bin, which is moved in steps of 0.1 K throughout the temperature space to obtain the continuous local slope of the point cloud (sketched out in SM Fig. 2a). We decompose the net TOA imbalance into its clear sky and cloud radiative effects (CRE; e.g., Wetherald and Manabe (1988); Soden and Held (2006); Ceppi and Gregory (2017)) in the shortwave and longwave (Fig. 2a). The feedbacks change continuously – not on obviously separable timescales – in some models more at the beginning of the simulations (e.g., CESM104), in some models after 150 years (e.g., GISS2R) or, in some models, intermittently throughout the simulation (e.g., MPIESM11 or HadGEM2). The shortwave CRE dominates the magnitude and the timing of the net feedback change, and can be counteracted by the longwave CRE. The reduction of the shortwave clear sky feedback associated with ice albedo, lapse rate, and water vapor is a function of temperature and occurs on centennial to millennial timescales. Longwave clear sky changes, when present, contribute to the increase of the sensitivity with equilibration time and temperature. The net feedback parameter can be composed of a subtle balance of different components at any time and the forced signal is not obviously linked to the feedback arising from internal variability, defined by regressing all available annual and global means of TOA imbalance and surface temperature anomalies (relative to the mean) of the control simulations (circles in Fig. 2a; Roe (2009); Brown et al. (2014); Zhou et al. (2015); Colman and Hanson (2017)).

Models which are more sensitive than other models – have feedbacks which are more positive – at the beginning of the simulation are generally also more sensitive towards the end. The model spread in the magnitude of feedbacks does not substantially reduce in time, while the feedback parameter change varies from negligible to an order of magnitude. We quantify the continuous changes across models by considering different time periods, namely years 1-20, 21-150, and 151-1000 (Fig. 2b), in each of which we regress all points. In addition to the increase of the feedback parameter between years 1-20 and 21-150, which has been documented for CMIP5 models (Geoffroy, Saint-Martin, Bellon, et al., 2013; Andrews et al., 2015; Proistosescu & Huybers, 2017; Ceppi & Gregory, 2017), there is a further increase from centennial to millennial timescales.

Previous research has shown that the change in feedbacks over time can come about through a dependence of feedback processes on the increasing temperature (Hansen et al., 1984; Jonko et al., 2013; Caballero & Huber, 2013; Meraner et al., 2013; Bloch-Johnson et al., 2015), due to evolving surface warming patterns and feedback processes (“pattern effect”;

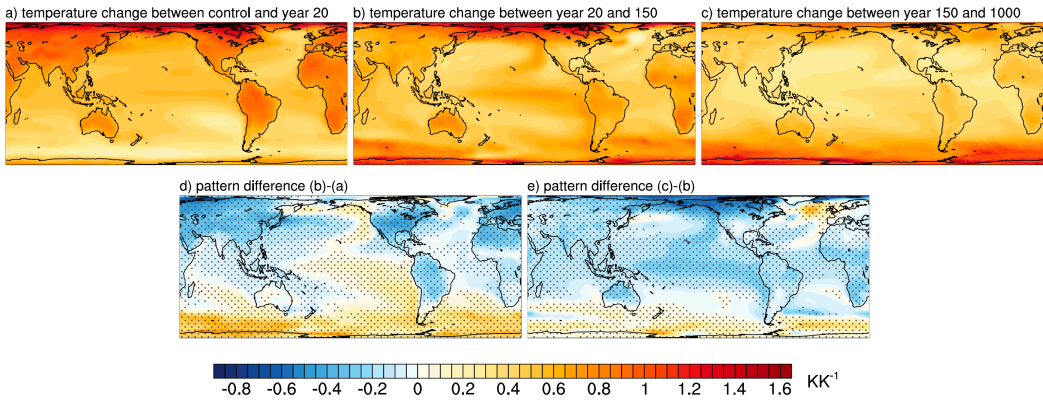


Figure 3. Multi-model mean normalized patterns of surface warming (local warming divided by global warming) between the average of (a) the control simulation and year 15-25, (b) year 15-25 and 140-160, (c) year 140-160 and 800-1000, and their differences (d and e) for the same models and simulations as in Fig. 2b. For models contributing several simulations, these are averaged. Stippling in panel d and e indicates that 9 out of 11 models agree in the sign of change.

Senior and Mitchell (2000); Winton et al. (2010); Armour et al. (2013); M. A. A. Rugenstein, Gregory, et al. (2016); Gregory and Andrews (2016); Haugstad et al. (2017); Paynter et al. (2018)), or both at the same time (Rohrschneider et al., 2019). There is no published method which clearly differentiates between time/pattern and temperature/state dependence and simulations with several forcing levels are needed to disentangle them. The relationship between forcing and CO₂ concentrations is a matter of debate (Etminan et al., 2016) and further complicates the analysis, as time, temperature, and forcing level dependence might compensate to some degree (Gregory et al., 2015). As not all models contributed several forcing levels, we focus in the following on robust pattern changes in surface temperatures and feedbacks, which occur in most or all simulations irrespective of their overall temperature anomaly or forcing level.

3 Pattern evolution of surface warming and feedbacks

The evolution of surface warming patterns during the decadal, centennial, and millennial periods displays a fast establishment of a land-sea warming contrast, Arctic amplification, and the delayed warming over the Southern Ocean that have been studied on annual to centennial timescales (Fig. 3; Senior and Mitchell (2000); Li et al. (2013); Collins et al. (2013); Armour et al. (2016)). Arctic amplification does not change substantially,

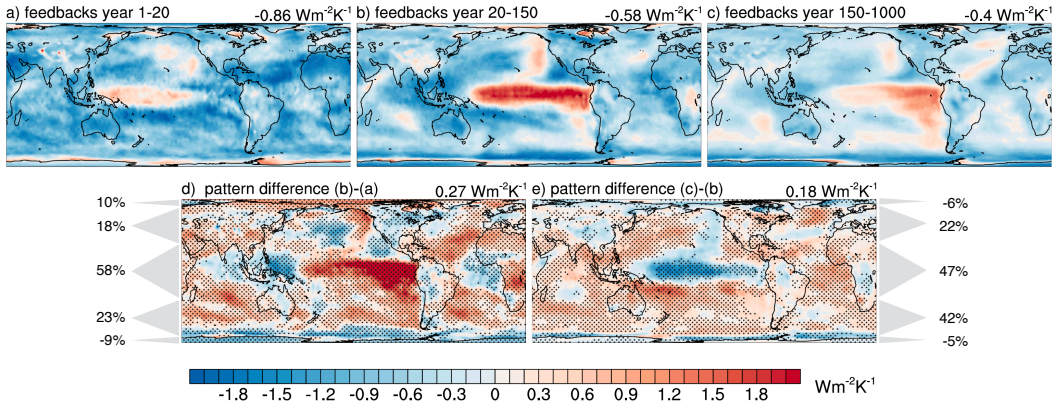


Figure 4. Time evolution of feedback patterns. Model-mean of local contribution to the change in global feedbacks (local TOA anomaly divided by global warming during the period indicated in the panel titles; see text for definitions) (a–c) and their differences (d, e). The global feedback value is shown in the panel title. Regionally aggregated contributions to the global values are indicated with percent numbers and gray triangles (22°S - 22°N , $22^{\circ}\text{S}/\text{N}$ - $66^{\circ}\text{S}/\text{N}$, $66^{\circ}\text{S}/\text{N}$ - $90^{\circ}\text{S}/\text{N}$, representing 40%, 27%, and 4% of the global surface area respectively). Model and simulations selection, weighting, and stippling is the same as in Fig. 3. SM Fig. 6–12 shows all TOA components.

whereas Antarctic amplification strengthens by approximately 50% on centennial to millennial timescales (Salzmann, 2017; M. Rugenstein et al., 2019). The warming in the northern North Atlantic reflects the strengthening of the Atlantic meridional overturning circulation, after the initial decline (Stouffer & Manabe, 2003; Li et al., 2013; M. A. A. Rugenstein, Sedláček, & Knutti, 2016; Rind et al., 2018; Jansen et al., 2018).

In the Pacific, at all times, the temperatures in absolute terms are higher in the West compared to the East Pacific. The eastern equatorial Pacific warms more than the warm pool in most simulations, a phenomenon reminiscent of the positive phase of the El-Niño-Southern-Oscillation (ENSO) (“ENSO-like warming” (Song & Zhang, 2014; Andrews et al., 2015; Luo et al., 2017; Tierney et al., 2019)). This tendency can last several millennia, but significantly reduces or stops in most simulations after a few hundred years. Similar to the Equatorial east Pacific, the south east Pacific warms more than the warm pool (Zhou et al., 2016; Andrews & Webb, 2018). However, models display a large variance in the timescales of warming in these two regions, i.e. the warm pool can initially warm faster or slower than the south east Pacific. Across the Pacific, the change in surface warming pattern is reminiscent of the Interdecadal Pacific Oscillation (IPO; Fig. 3d). In many models, the reduction

of the Walker circulation coincides with the decadal to centennial ENSO/IPO-like warming pattern, but it does not obviously coincide with surface warming pattern changes on the millennial timescale, indicating that subtropical ocean gyre advection and upwelling play a more prominent role on longer timescales (Knutson & Manabe, 1995; Song & Zhang, 2014; Fedorov et al., 2015; Andrews & Webb, 2018; Luo et al., 2017; Zhou et al., 2017; Kohyama et al., 2017). The mechanisms and spread of model responses in the Pacific are still under investigation.

Feedbacks defined as the local tangent in temperature-TOA space as used in Fig. 2a contain a signal from both the internal variability and the forced response. In order to isolate the forced response, we take the difference of the means at the beginning and end of the time periods discussed above. We call this definition of feedbacks the *finite difference approach*, as it represents a change *across* a time period (SM Fig. 2b). Fig. 4 shows the local contribution to the global net TOA changes (defined as the local change in TOA imbalance divided by the global temperature change.) for the same time periods and models as used in Fig. 3. In the initial years, the atmosphere restores radiative balance through increased radiation to space almost everywhere, except in the western-central Pacific (Fig. 4a), whereas on decadal to centennial timescales, the structure of the feedbacks mirrors the surface temperature evolution and develops a pattern reminiscent of ENSO/IPO (Fig. 4b). The cloud response dominates the pattern change, although for CMIP5 models, changes on decadal and centennial timescales have been attributed to changing lapse rate feedbacks as well (SM Fig. 6-8 and Andrews et al. (2015); Andrews and Webb (2018); Ceppi and Gregory (2017)). For the millennial timescales, our models show that feedbacks become less negative almost everywhere, switching from slightly negative to positive in parts of the Southern Ocean and North Atlantic region, and become less destabilizing in the Tropical Pacific (Fig. 4c). The feedback pattern change from decadal to centennial timescales (Fig. 4d) is reversed in many regions on centennial to millennial timescales (Fig. 4e), particularly in the entire Pacific basin, the Atlantic, and parts of Asia and North America. This “pattern flip” is dominated by longwave CRE (SM Fig. 8) and mirrors, in the Pacific, the reduction in ENSO/IPO-like surface warming patterns discussed for the surface temperature evolution.

Note that the local temperature is not part of the calculation of the local contribution in feedback changes. Due to the far-field effects of local feedbacks (e.g., Rose et al. (2014); Kang and Xie (2014); M. A. A. Rugenstein, Caldeira, and Knutti (2016); Zhou et al. (2016, 2017); Ceppi and Gregory (2017); Liu et al. (2018); Dong et al. (2019)), the relation between

the local feedback contribution (Fig. 4) and the local temperatures (Fig. 3) is not straightforward. There is strong correspondence between changes of TOA fluxes and temperature patterns in the Pacific on decadal to millennial timescales: Stronger (weaker) local warming coincides with a more positive (negative) local feedback contribution. However, there is no clear correspondence directly after the application of the forcing, or over land and the Southern Ocean through time. SM Fig. 13 and 14 show overlays of Fig. 3 and 4 for a better comparison. A local correspondence does not necessarily indicate a strong local feedback (i.e. local TOA divided by local surface temperature change), as both the local TOA and the surface in one region could be forced by another region. A closer investigation of local and far-field influence of feedbacks is under investigation (Bloch-Johnson et al., in revision).

Although the spatial patterns of changing temperature and radiative feedbacks vary among models, the large scale features discussed here occur robustly across most models and forcing levels, and also occur in the *1pct2x* and *1pct4x* simulations, which are not included in the figures.

4 Regions accounting for changing global feedbacks

We quantify the contribution of the tropics, extra-tropics, and polar regions to the global feedback change (Fig. 4d,e) by adding up all feedback contributions of the respective areas indicated by the gray triangles and expressing them as percentages of the total. We note that the total is the global feedback parameter, i.e., the slope of the point clouds in Fig. 1 which is indicated on the top right of each panel. These percentages reflect the role played by TOA fluxes in each region, which is not the same as the role played by surface warming in each region, as noted above. Whereas the tropics account for the bulk of the change (58% on decadal to centennial and 47% on centennial to millennial timescales), the mid-latitudes become more important with time (Northern and Southern Hemisphere combined for 41% on decadal to centennial and for 66% on centennial to millennial timescales). The high latitudes, dominated by the shortwave clear sky feedback (SM Fig. 12), play only a minor role in influencing the global response at all timescales. The regional accounting of global feedback changes permits us to test competing explanations regarding the spatial feedback pattern by placing them in a common temporal framework. Primary regions controlling the global feedback evolution have been suggested to be the Southern Hemisphere mid to high latitudes (Senior & Mitchell, 2000), the Northern Hemisphere subpolar regions (Rose & Rayborn, 2016; Trossman et al., 2016), and the Tropics (Jonko et al., 2013; Mer-

258 aner et al., 2013; Block & Mauritsen, 2013; Andrews et al., 2015; Ceppi & Gregory, 2019),
259 especially in the Pacific (Andrews & Webb, 2018; Ceppi & Gregory, 2017).

260 The simulations robustly shows a delayed warming in the Southern Hemisphere relative
261 to the Northern Hemisphere throughout the millennia-long integrations, which correlates
262 with the time evolution of net TOA and shortwave CRE (not shown). This behavior lends
263 support to the hypothesis of Senior and Mitchell (2000) who propose that feedbacks change
264 through time due to the slow warming rates of the Southern Ocean relative to the upper
265 atmospheric levels. This reduced lapse rate increases atmospheric static stability (and thus,
266 the shortwave cloud response) in the transient part of the simulation, but decreasingly less
267 so towards equilibrium.

268 The extra-tropical cloud response in the model-mean is non-negligible in the Southern
269 Ocean and North Atlantic on decadal to centennial timescales, as proposed by Rose and
270 Rencurrel (2016) and Trossman et al. (2016). However, it comes to dominate the global
271 response only on centennial to millennial timescales and when both hemispheres are consid-
272 ered.

273 We find that the longwave clear sky feedback does moderately increase in many mod-
274 els as the temperature or the forcing level increases, mainly in the tropics and Northern
275 Hemisphere mid-latitudes (Fig. 2a, SM Fig. 4, SM Fig. 5). This is in accordance with the
276 proposed argument that the tropics govern the global feedback evolution because the water
277 vapor feedback increases with warming (Jonko et al., 2013; Meraner et al., 2013; Block &
278 Mauritsen, 2013; Andrews et al., 2015), possibly following the rising tropical tropopause
279 (Meraner et al., 2013; Mauritsen et al., 2018).

280 Recent work has focused on the relative influence of the Pacific, specifically the relative
281 influence of temperatures of the warm pool versus compared to other regions. Feedbacks in
282 regions of atmospheric deep convections have a far-field and global effect, while feedbacks
283 in regions of atmospheric subsidence have only a local or regional influence (Barsugli &
284 Sardeshmukh, 2002; Zhou et al., 2017; Andrews & Webb, 2018; Ceppi & Gregory, 2019;
285 Dong et al., 2019). With the available fields in the LongRunMIP archive, we cannot quan-
286 tify the relative importance of water vapor and lapse rate feedbacks. However, the short and
287 longwave cloud response (SM Fig. 6–8) in the models qualitatively agree with the proposed
288 change of tropospheric stability patterns on decadal to centennial timescales (Andrews &
289 Webb, 2018; Ceppi & Gregory, 2017), especially in the Pacific region. In contrast, on centen-

290 nial to millennial timescales, the tropical Pacific response becomes less important compared
291 to the mid-latitudes and the net tropical CRE does not change anymore (SM Fig. 6).

292 **5 Implications**

293 We demonstrate that the evolution of the global feedback response is dominated by the
294 mid-latitudes on centennial to millennial and the tropics on decadal to centennial timescales.
295 The global net feedback change is a result of a subtle balance of different regions and different
296 TOA components at all times; even more so in single simulations than in the model mean
297 shown here. This motivates process-based feedback studies in individual models as well
298 as multi-model ensembles to draw robust conclusions and increase physical understanding
299 of processes. To relate the timescales and model behavior to the observational record and
300 paleo proxies a better understanding of a) the atmospheric versus oceanic drivers of surface
301 temperature patters in both, the coupled climate models and the real world and b) the local
302 and far field interactions of tropospheric stability, clouds, and surface temperatures need
303 to be achieved. Note that climate models have typical and persistent biases in regions we
304 identify as important, mainly the Equatorial Pacific, Southern Ocean and ocean upwelling
305 regions. The pattern effect of the real world might act on timescales which are different
306 than the ones of the climate models.

307 Our results show that radiative feedbacks, usually called “fast”, act continuously less
308 stabilizing on the climate system as the models approach equilibrium. As a result, the
309 equilibrium warming is higher than estimated with common extrapolation methods from
310 short simulations for all models and simulations in the LongRunMIP archive. ECS has
311 been historically used as a model characterization (Charney et al., 1979), but some studies
312 propose that it is not the most adequate measure for estimating changes expected over the
313 next decades and until the end of the century (e.g., Otto et al. (2013); Shiogama et al. (2016);
314 Knutti et al. (2017)). Alternative climate sensitivity measures are the effective climate
315 sensitivity computed on different timescales, the transient climate response to gradually
316 increasing CO₂ (TCR), or the transient climate response to cumulative carbon emissions
317 (e.g., Allen and Frame (2007); Millar et al. (2015); Gregory et al. (2015); Grose et al. (2018)).
318 Beyond not being an accurate indicator of the equilibrium response, these alternative climate
319 sensitivity measures capture the models in different degrees of equilibration. We show that
320 it is an open question how different measures of sensitivity relate to each other. A recent
321 study shows that $\Delta T_{est\ 1-150}$ correlates better than TCR with end-of-21st-century warming

322 across model (Grose et al. (2018), see also Gregory et al. (2015)). Thus, we underscore
323 the need of comparing models, observations, and paleo proxies on well-defined measures of
324 climate sensitivity, which ensure they are in the same state of equilibration.

325 **Acknowledgments**

326 Fields shown in this paper can be accessed on <https://data.iac.ethz.ch/longrunmip/>
327 GRL/. See www.longrunmip.org and M. Rugenstein et al. (2019) for more details on each
328 simulation and available variables, not shown here.

329 We thank Urs Beyerle, Erich Fischer, Jeremy Rugenstein, Levi Silvers, and Martin Stolpe
330 for technical help and comments on the manuscript.

331 MR is funded by the Alexander von Humboldt Foundation. NCAR is a major facility spon-
332 sored by the U.S. National Science Foundation under Cooperative Agreement 1852977. TA
333 was supported by the Joint UK BEIS/Defra Met Office Hadley Centre Climate Programme
334 (GA01101). TLF acknowledges support from the Swiss National Science Foundation un-
335 der Grant PP00P2_170687, from the European Union’s Horizon 2020 research and innova-
336 tion program under grant agreement no. 821003 (CCiCC) CL was supported through the
337 Clusters of Excellence CliSAP (EXC177) and CLICCS (EXC2037), University Hamburg,
338 funded through the German Research Foundation (DFG). SY was partly supported by Eu-
339 ropean Research Council under the European Community’s Seventh Framework Programme
340 (FP7/20072013)/ERC grant agreement 610055 as part of the ice2ice project.

341 **References**

- 342 Allen, M. R., & Frame, D. J. (2007). Call off the quest. *Science*, 318(5850), 582-583.
 343 Retrieved from <http://www.sciencemag.org/content/318/5850/582.short> doi:
 344 10.1126/science.1149988
- 345 Andrews, T., Gregory, J. M., & Webb, M. J. (2015). The Dependence of Radiative Forcing
 346 and Feedback on Evolving Patterns of Surface Temperature Change in Climate Models.
 347 *Journal of Climate*, 28(4), 1630-1648. Retrieved from <http://dx.doi.org/10.1175/JCLI-D-14-00545.1>
- 348 Andrews, T., Gregory, J. M., Webb, M. J., & Taylor, K. E. (2012). Forcing, feedbacks and cli-
 349 mate sensitivity in CMIP5 coupled atmosphere-ocean climate models. *Geophysical Re-
 350 search Letters*, 39(9). Retrieved from <http://dx.doi.org/10.1029/2012GL051607>
- 351 Andrews, T., & Webb, M. J. (2018). The Dependence of Global Cloud and Lapse Rate
 352 Feedbacks on the Spatial Structure of Tropical Pacific Warming. *Journal of Climate*,
 353 31(2), 641-654. Retrieved from <https://doi.org/10.1175/JCLI-D-17-0087.1>
- 354 Armour, K. C. (2017). Energy budget constraints on climate sensitivity in light of inconstant
 355 climate feedbacks. *Nature Climate Change*, 7, 331 EP -. Retrieved from <http://dx.doi.org/10.1038/nclimate3278>
- 356 Armour, K. C., Bitz, C. M., & Roe, G. H. (2013). Time-Varying Climate Sensitivity
 357 from Regional Feedbacks. *Journal of Climate*, 26(13), 4518–4534. Retrieved from
 358 <http://dx.doi.org/10.1175/JCLI-D-12-00544.1>
- 359 Armour, K. C., Marshall, J., Scott, J. R., Donohoe, A., & Newsom, E. R. (2016). Southern
 360 ocean warming delayed by circumpolar upwelling and equatorward transport. *Nature
 361 Geosci*, 9(7), 549–554. Retrieved from <http://dx.doi.org/10.1038/ngeo2731>
- 362 Barsugli, J. J., & Sardeshmukh, P. D. (2002). Global atmospheric sensitivity to tropical sst
 363 anomalies throughout the indo-pacific basin. *Journal of Climate*, 15(23), 3427-3442.
 364 Retrieved from [https://doi.org/10.1175/1520-0442\(2002\)015<3427:GASTTS>2.0.CO;2](https://doi.org/10.1175/1520-0442(2002)015<3427:GASTTS>2.0.CO;2)
- 365 Bloch-Johnson, J., Pierrehumbert, R. T., & Abbot, D. S. (2015). Feedback tempera-
 366 ture dependence determines the risk of high warming. *Geophysical Research Letters*,
 367 42(12), 4973– 4980. Retrieved from [\(2015GL064240\)](http://dx.doi.org/10.1002/2015GL064240)
- 368 Bloch-Johnson, J., Rugenstein, M., & Abbot, D. S. (in revision). Spatial radiative feedbacks
 369 from interannual variability using multiple regression. *Journal of Climate*.
- 370

- 374 Block, K., & Mauritsen, T. (2013). Forcing and feedback in the MPI-ESM-LR coupled model
375 under abruptly quadrupled CO₂. *Journal of Advances in Modeling Earth Systems*,
376 5(4), 676–691. Retrieved from <http://dx.doi.org/10.1002/jame.20041>
- 377 Brant, F., & Schneider, T. (2016). Constraints on Climate Sensitivity from Space-Based
378 Measurements of Low-Cloud Reflection. *Journal of Climate*, 29(16), 5821–5835. Re-
379 tried from <https://doi.org/10.1175/JCLI-D-15-0897.1>
- 380 Brown, P. T., Li, W., Li, L., & Ming, Y. (2014). Top-of-atmosphere radiative contribution
381 to unforced decadal global temperature variability in climate models. *Geophysical*
382 *Research Letters*, 41(14), 5175–5183. Retrieved from <http://dx.doi.org/10.1002/2014GL060625>
- 384 Caballero, R., & Huber, M. (2013). State-dependent climate sensitivity in past warm
385 climates and its implications for future climate projections. *Proceedings of the National*
386 *Academy of Sciences of the United States of America*, 110(35), 14162–14167. Retrieved
387 from <http://www.ncbi.nlm.nih.gov/pmc/articles/PMC3761583/>
- 388 Calel, R., & Stainforth, D. A. (2017). On the Physics of Three Integrated Assessment
389 Models. *Bulletin of the American Meteorological Society*, 98(6), 1199–1216. Retrieved
390 from <https://doi.org/10.1175/BAMS-D-16-0034.1>
- 391 Ceppi, P., & Gregory, J. M. (2017). Relationship of tropospheric stability to climate
392 sensitivity and earth's observed radiation budget. *Proceedings of the National Academy*
393 *of Sciences*, 114(50), 13126–13131. Retrieved from <https://www.pnas.org/content/114/50/13126>
- 395 Ceppi, P., & Gregory, J. M. (2019). A refined model for the Earth's global energy balance.
396 *Climate Dynamics*. Retrieved from <https://doi.org/10.1007/s00382-019-04825-x>
- 398 Charney, J., Arakawa, A., Baker, D., Bolin, B., Dickinson, R. E., Goody, R., ... Wunsch,
399 C. (1979). *Carbon Dioxide and Climate: A Scientific Assessment* (Tech. Rep.).
400 Washington, DC.: National Academy of Science.
- 401 Collins, M., Knutti, R., Arblaster, J. M., Dufresne, J.-L., Fichefet, T., Friedlingstein, P., ...
402 Wehner, M. F. (2013). Long-term Climate Change: Projections, Commitments and
403 Irreversibility. In T. Stocker et al. (Eds.), Cambridge University Press, Cambridge,
404 United Kingdom and New York, NY, USA.
- 405 Colman, R., & Hanson, L. (2017). On the relative strength of radiative feedbacks under
406 climate variability and change. *Climate Dynamics*, 49(5), 2115–2129. Retrieved from

- 407 <https://doi.org/10.1007/s00382-016-3441-8>
- 408 Dong, Y., Proistosescu, C., Armour, K. C., & Battisti, D. S. (2019). Attributing Historical
409 and Future Evolution of Radiative Feedbacks to Regional Warming Patterns using
410 a Green's Function Approach: The Preeminence of the Western Pacific. *Journal of*
411 *Climate*, 0(0), null. Retrieved from <https://doi.org/10.1175/JCLI-D-18-0843.1>
- 412 Etminan, M., Myhre, G., Highwood, E. J., & Shine, K. P. (2016). Radiative forcing
413 of carbon dioxide, methane, and nitrous oxide: A significant revision of the methane
414 radiative forcing. *Geophysical Research Letters*, 43(24), 12,614–12,623. Retrieved from
415 <https://agupubs.onlinelibrary.wiley.com/doi/abs/10.1002/2016GL071930>
- 416 Eyring, V., Bony, S., Meehl, G. A., Senior, C. A., Stevens, B., Stouffer, R. J., & Taylor, K. E.
417 (2016). Overview of the Coupled Model Intercomparison Project Phase 6 (CMIP6)
418 experimental design and organization. *Geoscientific Model Development*, 9(5), 1937–
419 1958. Retrieved from <https://www.geosci-model-dev.net/9/1937/2016/>
- 420 Fedorov, A. V., Burles, N. J., Lawrence, K. T., & Peterson, L. C. (2015). Tightly linked
421 zonal and meridional sea surface temperature gradients over the past five million
422 years. *Nature Geoscience*, 8, 975 EP -. Retrieved from <https://doi.org/10.1038/ngeo2577>
- 424 Flato, G., Marotzke, J., Abiodun, B., Braconnot, P., Chou, S., Collins, W., ... Rum-
425 mukainen, M. (2013). Evaluation of Climate Models. In T. Stocker et al. (Eds.),
426 Cambridge University Press, Cambridge, United Kingdom and New York, NY, USA.
- 427 Forster, P. M. (2016). Inference of climate sensitivity from analysis of earth's energy
428 budget. *Annual Review of Earth and Planetary Sciences*, 44(1), 85–106. Retrieved
429 from <http://dx.doi.org/10.1146/annurev-earth-060614-105156>
- 430 Geoffroy, O., Saint-Martin, D., Bellon, G., Volodire, A., Olivié, D., & Tytéca, S. (2013).
431 Transient Climate Response in a Two-Layer Energy-Balance Model. Part II: Rep-
432 resentation of the Efficacy of Deep-Ocean Heat Uptake and Validation for CMIP5
433 AOGCMs. *Journal of Climate*, 26(6), 1859–1876. Retrieved from <http://dx.doi.org/10.1175/JCLI-D-12-00196.1>
- 435 Geoffroy, O., Saint-Martin, D., Olivié, D. J. L., Volodire, A., Bellon, G., & Tytéca, S.
436 (2013). Transient Climate Response in a Two-Layer Energy-Balance Model. Part I:
437 Analytical Solution and Parameter Calibration Using CMIP5 AOGCM Experiments.
438 *Journal of Climate*, 26(6), 1841–1857. Retrieved from <http://dx.doi.org/10.1175/JCLI-D-12-00195.1>

- 440 Good, P., Andrews, T., Chadwick, R., Dufresne, J.-L., Gregory, J. M., Lowe, J. A., ...
441 Shiogama, H. (2016). nonlinMIP contribution to CMIP6: model intercomparison
442 project for non-linear mechanisms: physical basis, experimental design and analysis
443 principles (v1.0). *Geoscientific Model Development*, 9(11), 4019–4028. Retrieved from
444 <https://www.geosci-model-dev.net/9/4019/2016/>
- 445 Good, P., Lowe, J. A., Andrews, T., Wiltshire, A., Chadwick, R., Ridley, J. K., ... Sh-
446 iogama, H. (2015, 02). Nonlinear regional warming with increasing co2 concentrations.
447 *Nature Clim. Change*, 5(2), 138–142.
- 448 Gregory, J. M., & Andrews, T. (2016). Variation in climate sensitivity and feedback param-
449 eters during the historical period. *Geophysical Research Letters*, 43(8), 3911–3920.
450 Retrieved from <http://dx.doi.org/10.1002/2016GL068406>
- 451 Gregory, J. M., Andrews, T., & Good, P. (2015). The inconstancy of the transient
452 climate response parameter under increasing CO₂. *Philosophical Transactions of*
453 *the Royal Society of London A: Mathematical, Physical and Engineering Sciences*,
454 373(2054). Retrieved from <http://rsta.royalsocietypublishing.org/content/373/2054/20140417>
- 456 Gregory, J. M., Ingram, W. J., Palmer, M. A., Jones, G. S., Stott, P. A., Thorpe, R. B., ...
457 Williams, K. D. (2004). A new method for diagnosing radiative forcing and climate
458 sensitivity. *Geophysical Research Letters*, 31(3). Retrieved from <http://dx.doi.org/10.1029/2003GL018747>
- 460 Grose, M. R., Gregory, J., Colman, R., & Andrews, T. (2018). What Climate Sensitivity
461 Index Is Most Useful for Projections? *Geophysical Research Letters*, 45(3), 1559–1566.
462 Retrieved from <http://dx.doi.org/10.1002/2017GL075742>
- 463 Hansen, J., Lacis, A., Rind, D., Russel, G., Stone, P., Fung, I., ... Lerner, J. (1984).
464 Analysis of feedback mechanisms. In: Climate processes and climate sensitivity. In
465 J. Hansen & T. Takahashi (Eds.), *Climate sensitivity: Analysis of feedback mecha-*
466 *nisms* (Vol. 5, pp. 130–163). American Geophysical Union, Washington, DC: AGU
467 Geophysical Monograph 29, Maurice Ewing.
- 468 Hargreaves, J. C., & Annan, J. D. (2016). Could the pliocene constrain the equilibrium
469 climate sensitivity? *Climate of the Past*, 12(8), 1591–1599. Retrieved from <http://www.clim-past.net/12/1591/2016/>
- 471 Haugstad, A. D., Armour, K. C., Battisti, D. S., & Rose, B. E. J. (2017). Relative roles
472 of surface temperature and climate forcing patterns in the inconstancy of radiative

- 473 feedbacks. *Geophysical Research Letters*, 44(14), 7455-7463. Retrieved from <https://agupubs.onlinelibrary.wiley.com/doi/abs/10.1002/2017GL074372>
- 474
- 475 Houghton, J., Jenkins, G. J., & Ephraums, J. J. (1990). Report prepared for Intergovernmental Panel on Climate Change by Working Group I. In *Climate Change: The IPCC Scientific Assessment* (p. 410). Cambridge University Press.
- 476
- 477
- 478 Jansen, M. F., Nadeau, L.-P., & Merlis, T. M. (2018). Transient versus Equilibrium Response of the Ocean's Overturning Circulation to Warming. *Journal of Climate*, 31(13), 5147-5163. Retrieved from <https://doi.org/10.1175/JCLI-D-17-0797.1>
- 479
- 480
- 481 Jonko, A. K., Shell, K. M., Sanderson, B. M., & Danabasoglu, G. (2013). Climate Feedbacks in CCSM3 under Changing CO₂ Forcing. Part II: Variation of Climate Feedbacks and Sensitivity with Forcing. *Journal of Climate*, 26(9), 2784-2795. Retrieved from <http://dx.doi.org/10.1175/JCLI-D-12-00479.1>
- 482
- 483
- 484
- 485 Kang, S. M., & Xie, S.-P. (2014). Dependence of Climate Response on Meridional Structure of External Thermal Forcing. *Journal of Climate*, 27(14), 5593-5600. Retrieved from <http://dx.doi.org/10.1175/JCLI-D-13-00622.1>
- 486
- 487
- 488 Knutson, T. R., & Manabe, S. (1995). Time-Mean Response over the Tropical Pacific to Increased C0₂ in a Coupled Ocean-Atmosphere Model. *Journal of Climate*, 8(9), 2181-2199. Retrieved from [https://doi.org/10.1175/1520-0442\(1995\)008<2181:TMROTT>2.0.CO;2](https://doi.org/10.1175/1520-0442(1995)008<2181:TMROTT>2.0.CO;2)
- 489
- 490
- 491
- 492 Knutti, R., & Rugenstein, M. A. A. (2015). Feedbacks, climate sensitivity and the limits of linear models. *Philosophical Transactions of the Royal Society of London A: Mathematical, Physical and Engineering Sciences*, 373(2054). doi: 10.1098/rsta.2015.0146
- 493
- 494
- 495 Knutti, R., Rugenstein, M. A. A., & Hegerl, G. C. (2017). Beyond equilibrium climate sensitivity. *Nature Geoscience*, 10, 727 EP -. Retrieved from <http://dx.doi.org/10.1038/ngeo3017>
- 496
- 497
- 498 Kohyama, T., Hartmann, D. L., & Battisti, D. S. (2017). La Nina-like Mean-State Response to Global Warming and Potential Oceanic Roles. *Journal of Climate*, 30(11), 4207-4225. Retrieved from <https://doi.org/10.1175/JCLI-D-16-0441.1>
- 499
- 500
- 501 Lewis, N., & Curry, J. A. (2015). The implications for climate sensitivity of AR5 forcing and heat uptake estimates. *Climate Dynamics*, 45(3), 1009-1023. Retrieved from <http://dx.doi.org/10.1007/s00382-014-2342-y>
- 502
- 503
- 504 Li, C., Storch, J.-S., & Marotzke, J. (2013). Deep-ocean heat uptake and equilibrium climate response. *Climate Dynamics*, 40(5-6), 1071-1086. Retrieved from <http://>
- 505

- 506 dx.doi.org/10.1007/s00382-012-1350-z
- 507 Liu, F., Lu, J., Garuba, O. A., Huang, Y., Leung, L. R., Harrop, B. E., & Luo, Y. (2018).
508 Sensitivity of Surface Temperature to Oceanic Forcing via q-Flux Green's Function
509 Experiments. Part II: Feedback Decomposition and Polar Amplification. *Journal of*
510 *Climate*, 31(17), 6745-6761. Retrieved from <https://doi.org/10.1175/JCLI-D-18-0042.1>
- 512 Luo, Y., Lu, J., Liu, F., & Garuba, O. (2017). The Role of Ocean Dynamical Thermostat in
513 Delaying the El Niño-Like Response over the Equatorial Pacific to Climate Warming.
514 *Journal of Climate*, 30(8), 2811-2827. Retrieved from <https://doi.org/10.1175/JCLI-D-16-0454.1>
- 516 Mauritsen, T., Bader, J., Becker, T., Behrens, J., Bittner, M., Brokopf, R., ... Roeck-
517 ner, E. (2018). Developments in the mpi-m earth system model version 1.2 (mpi-
518 esm 1.2) and its response to increasing co2. *Journal of Advances in Modeling Earth*
519 *Systems*, 0(ja). Retrieved from <https://agupubs.onlinelibrary.wiley.com/doi/abs/10.1029/2018MS001400>
- 521 Meraner, K., Mauritsen, T., & Voigt, A. (2013). Robust increase in equilibrium climate
522 sensitivity under global warming. *Geophysical Research Letters*, 40(22), 5944-5948.
523 Retrieved from <http://dx.doi.org/10.1002/2013GL058118>
- 524 Millar, R. J., Otto, A., Forster, P. M., Lowe, J. A., Ingram, W. J., & Allen, M. R. (2015).
525 Model structure in observational constraints on transient climate response. *Climatic*
526 *Change*, 131(2), 199-211. Retrieved from <https://doi.org/10.1007/s10584-015-1384-4>
- 528 Murphy, J. M. (1995). Transient Response of the Hadley Centre Coupled Ocean-Atmosphere
529 Model to Increasing Carbon Dioxide. Part 1: Control Climate and Flux Adjustment.
530 *Journal of Climate*, 8(1), 36-56. Retrieved from [http://dx.doi.org/10.1175/1520-0442\(1995\)008<0036:TROTHC>2.0.CO;2](http://dx.doi.org/10.1175/1520-0442(1995)008<0036:TROTHC>2.0.CO;2)
- 532 Myhre, G., Highwood, E. J., Shine, K. P., & Stordal, F. (1998). New estimates of radiative
533 forcing due to well mixed greenhouse gases. *Geophysical Research Letters*, 25(14),
534 2715-2718. Retrieved from <https://agupubs.onlinelibrary.wiley.com/doi/abs/10.1029/98GL01908>
- 536 Otto, A., Otto, F. E. L., Boucher, O., Church, J., Hegerl, G., Forster, P. M., ... Allen,
537 M. R. (2013). Energy budget constraints on climate response. *Nature Geosci*, 6(6),
538 415-416. Retrieved from <http://dx.doi.org/10.1038/ngeo1836>

- 539 Paynter, D., Frölicher, T. L., Horowitz, L. W., & Silvers, L. G. (2018). Equilibrium Cli-
540 mate Sensitivity Obtained From Multimillennial Runs of Two GFDL Climate Models.
541 *Journal of Geophysical Research: Atmospheres*, 123(4), 1921-1941. Retrieved from
542 <https://agupubs.onlinelibrary.wiley.com/doi/abs/10.1002/2017JD027885>
- 543 Proistosescu, C., & Huybers, P. J. (2017). Slow climate mode reconciles historical and
544 model-based estimates of climate sensitivity. *Science Advances*, 3(7). Retrieved from
545 <http://advances.sciencemag.org/content/3/7/e1602821>
- 546 Rind, D., Schmidt, G. A., Jonas, J., Miller, R., Nazarenko, L., Kelley, M., & Romanski,
547 J. (2018). Multicentury Instability of the Atlantic Meridional Circulation in Rapid
548 Warming Simulations With GISS ModelE2. *Journal of Geophysical Research: At-*
549 *mospheres*, 123(12), 6331-6355. Retrieved from <https://agupubs.onlinelibrary.wiley.com/doi/abs/10.1029/2017JD027149>
- 551 Roe, G. (2009). Feedbacks, timescales, and seeing red. *Annual Review of Earth and*
552 *Planetary Sciences*, 37(1), 93-115. Retrieved from <http://dx.doi.org/10.1146/annurev.earth.061008.134734>
- 554 Rohrschneider, T., Stevens, B., & Mauritsen, T. (2019, 02). On simple representations of
555 the climate response to external radiative forcing. *Climate Dynamics*. doi: 10.1007/s00382-019-04686-4
- 557 Rose, B. E. J., Armour, K. C., Battisti, D. S., Feldl, N., & Koll, D. D. B. (2014). The
558 dependence of transient climate sensitivity and radiative feedbacks on the spatial pat-
559 tern of ocean heat uptake. *Geophysical Research Letters*, 41(3), 1071–1078. Retrieved
560 from <http://dx.doi.org/10.1002/2013GL058955>
- 561 Rose, B. E. J., & Rayborn, L. (2016). The Effects of Ocean Heat Uptake on Transient
562 Climate Sensitivity. *Current Climate Change Reports*, 1–12. Retrieved from <http://dx.doi.org/10.1007/s40641-016-0048-4>
- 564 Rose, B. E. J., & Rencurrel, M. C. (2016). The Vertical Structure of Tropospheric Water
565 Vapor: Comparing Radiative and Ocean-Driven Climate Changes. *Journal of Climate*,
566 29(11), 4251-4268. Retrieved from <http://dx.doi.org/10.1175/JCLI-D-15-0482.1>
- 568 Rugenstein, M., Bloch-Johnson, J., Abe-Ouchi, A., Andrews, T., Beyerle, U., Cao, L., ...
569 Yang, S. (2019). LongRunMIP – motivation and design for a large collection of
570 millennial-length GCM simulations. *Bulletin of the American Meteorological Society*,
571 0(0), null. Retrieved from <https://doi.org/10.1175/BAMS-D-19-0068.1>

- 572 Rugenstein, M. A. A., Caldeira, K., & Knutti, R. (2016). Dependence of global radiative
573 feedbacks on evolving patterns of surface heat fluxes. *Geophysical Research Letters*,
574 43(18), 9877–9885. Retrieved from <http://dx.doi.org/10.1002/2016GL070907>
- 575 Rugenstein, M. A. A., Gregory, J. M., Schaller, N., Sedláček, J., & Knutti, R. (2016). Mul-
576 tiannual Ocean–Atmosphere Adjustments to Radiative Forcing. *Journal of Climate*,
577 29(15), 5643–5659. Retrieved from <http://dx.doi.org/10.1175/JCLI-D-16-0312>
578 .1
- 579 Rugenstein, M. A. A., Sedláček, J., & Knutti, R. (2016). Nonlinearities in patterns of
580 long-term ocean warming. *Geophysical Research Letters*, 43(7), 3380–3388. Retrieved
581 from <http://dx.doi.org/10.1002/2016GL068041>
- 582 Salzmann, M. (2017). The polar amplification asymmetry: role of Antarctic surface height.
583 *Earth System Dynamics*, 8(2), 323–336. Retrieved from <https://www.earth-syst->
584 [dynam.net/8/323/2017/](https://www.earth-syst-dynam.net/8/323/2017/)
- 585 Senior, C. A., & Mitchell, J. F. B. (2000). The time-dependence of climate sensitivity.
586 *Geophysical Research Letters*, 27(17), 2685–2688. Retrieved from <http://dx.doi.org/10.1029/2000GL011373>
- 587 Shiogama, H., Stone, D., Emori, S., Takahashi, K., Mori, S., Maeda, A., ... Allen, M. R.
588 (2016). Predicting future uncertainty constraints on global warming projections. *Sci-*
589 *entific Reports*, 6, 18903 EP -.
- 590 Soden, B. J., & Held, I. M. (2006). An Assessment of Climate Feedbacks in Coupled
591 Ocean-Atmosphere Models. *Journal of Climate*, 19(14), 3354–3360. Retrieved from
592 <http://dx.doi.org/10.1175/JCLI3799.1>
- 593 Song, X., & Zhang, G. J. (2014). Role of Climate Feedback in El Niño-like SST Response to
594 Global Warming. *Journal of Climate*. Retrieved from <http://dx.doi.org/10.1175/JCLI-D-14-00072.1>
- 595 Stocker, T. F. e. a. (2013). *Climate Change 2013: The Physical Science Basis*. Cambridge
596 University Press, Cambridge, United Kingdom and New York, NY, USA.
- 597 Stouffer, R., & Manabe, S. (2003). Equilibrium response of thermohaline circulation to
598 large changes in atmospheric CO₂ concentration. *Climate Dynamics*, 20(7-8), 759–
599 773. Retrieved from <http://dx.doi.org/10.1007/s00382-002-0302-4>
- 600 Taylor, K. E., Stouffer, R. J., & Meehl, G. A. (2011). An Overview of CMIP5 and the
601 Experiment Design. *Bulletin of the American Meteorological Society*, 93(4), 485–498.
602 Retrieved from <http://dx.doi.org/10.1175/BAMS-D-11-00094.1>
- 603
- 604

- 605 Tian, B. (2015). Spread of model climate sensitivity linked to double-intertropical conver-
606 gence zone bias. *Geophysical Research Letters*, 42(10), 4133–4141. Retrieved from
607 <http://dx.doi.org/10.1002/2015GL064119>
- 608 Tierney, J. E., Haywood, A. M., Feng, R., Bhattacharya, T., & Otto-Bliesner, B. L. (2019).
609 Pliocene Warmth Consistent With Greenhouse Gas Forcing. *Geophysical Research
Letters*, 46(15), 9136-9144. Retrieved from <https://agupubs.onlinelibrary.wiley.com/doi/abs/10.1029/2019GL083802>
- 610 611
- 612 Trossman, D. S., Palter, J. B., Merlis, T. M., Huang, Y., & Xia, Y. (2016). Large-scale ocean
613 circulation-cloud interactions reduce the pace of transient climate change. *Geophysical
Research Letters*, 43(8), 3935–3943. Retrieved from <http://dx.doi.org/10.1002/2016GL067931>
- 614 615
- 616 Wetherald, R. T., & Manabe, S. (1988). Cloud feedback processes in a general circula-
617 tion model. *Journal of the Atmospheric Sciences*, 45(8), 1397–1416. Retrieved from
618 [http://dx.doi.org/10.1175/1520-0469\(1988\)045<1397:CFPIAG>2.0.CO;2](http://dx.doi.org/10.1175/1520-0469(1988)045<1397:CFPIAG>2.0.CO;2)
- 619 620
- 621 Winton, M., Takahashi, K., & Held, I. M. (2010). Importance of Ocean Heat Uptake Efficacy
622 to Transient Climate Change. *Journal of Climate*, 23(9), 2333-2344. Retrieved from
623 <http://dx.doi.org/10.1175/2009JCLI3139.1>
- 624 625
- 626 Zhou, C., Zelinka, M. D., Dessler, A. E., & Klein, S. A. (2015). The relationship between
627 inter-annual and long-term cloud feedbacks. *Geophysical Research Letters*. Retrieved
628 from <http://dx.doi.org/10.1002/2015GL066698> (2015GL066698)
- 629 630
- 631 Zhou, C., Zelinka, M. D., & Klein, S. A. (2016). Impact of decadal cloud variations on
the Earth's energy budget. *Nature Geosci*, 9(12), 871–874. Retrieved from <http://dx.doi.org/10.1038/ngeo2828>
- 632 633
- 634 Zhou, C., Zelinka, M. D., & Klein, S. A. (2017). Analyzing the dependence of global
635 cloud feedback on the spatial pattern of sea surface temperature change with a green's
636 function approach. *Journal of Advances in Modeling Earth Systems*, 9(5), 2174–2189.
637 Retrieved from <http://dx.doi.org/10.1002/2017MS001096>
- 638 639